The electronic structure of the mixed valence compound Pb3O4

Groot, R.A. de; Haas, C.; deGroot, R.A.

Published in:
Journal of Physics and Chemistry of Solids

DOI:
10.1016/S0022-3697(96)00165-5

Publication date:
1997

Pergamon

PII: S0022-3697(96)00165-8

J. Phys. Chem Solids Vol 58, No. 4, pp. 561-566, 1997

0022-3697/97 $17.00 + 0.00

THE ELECTRONIC STRUCTURE OF THE MIXED VALENCE COMPOUND Pb_3O_4

H. J. TERPSTRA, R. A. DE GROOT and C. HAAS

Laboratory of Chemical Physics, Materials Science Centre, University of Groningen, Nijenborgh 4, 9747 AG Groningen, The Netherlands

(*Received* 17 *July* 1996; *accepted* 23 *August* 1996)

Abstract—*Ab initio* self-consistent calculations of the electronic structure of Pb_3O_4 are presented. The calculations show that Pb_3O_4 is a semiconductor. The calculated bandgap of 1.1 eV is smaller than the observed gap of 2.1–2.2 eV. The calculations show strong hybridization between Pb(6s) and O(2p) states. For one type of lead atom, this leads to a distribution of Pb(6s) states over two occupied energy bands, similar to the situation in PbO. For the other type of lead atom in Pb_3O_4 the Pb(6s) states are distributed over an occupied and an unoccupied band, similar to the situation in β-PbO_2. This clearly demonstrates that Pb_3O_4 is a mixed valence compound, i.e. $Pb(II)_2Pb(IV)O_4$. According to the calculations, the conductivity of p-type Pb_3O_4 is due to holes in a Pb(II)(6s) valence band and the conductivity in *n*-type Pb_3O_4 is due to electrons in a Pb(IV)(6s) conduction band.

Keywords: A. oxides, A. semiconductors, D. electronic structure

1. INTRODUCTION

Trilead tetroxide Pb_3O_4 is a bright orange–red compound which occurs naturally as the mineral minium. Pb_3O_4 was historically used as a paint and the word miniature for illustrations in old manuscripts is derived from minium. More recently, Pb_3O_4 has been used in batteries and ceramics and was also widely used in corrosion resistant oil-based paints. With iron, the oxidizer Pb_3O_4 forms a layer of (Pb, Fe) oxides, which do not oxidize further. For environmental reasons Pb_3O_4 is now mostly replaced by other corrosion resistant compounds.

Although Pb_3O_4 is technologically a very important material, little is known about its physical properties. Pb_3O_4 is a semiconductor with a high resistivity, $\rho \sim 10^8\ \Omega$.cm for a pressed powder [1] and $\rho \sim 10^4\ \Omega$.cm for a Pb_3O_4 film [2]. The infrared spectra show the presence of Pb–O vibrations between 300 and 700 cm^{-1} [3] and for the dielectric constant, values between 13 and 17 have been reported [4, 5]. The bandgap was measured by reflectance and photovoltage technique [6–11]; the spectra show an absorption edge, indicating a bandgap of 2.1–2.2 eV. Benschop [12, 13] measured nuclear magnetic resonance spectra of lead oxides; for Pb_3O_4 two signals were observed, one similar to the signal observed for PbO and one similar to the signal observed for the insulator $SrPbO_3$.

Several authors have reported photoelectron spectra of Pb_3O_4. Kim *et al.* [14] deconvoluted the Pb 4f peaks into two peaks with an intensity ratio of 1:2, with the most intense peak at the highest binding energy and suggested that the two peaks are due to the two types of Pb atoms in Pb_3O_4. In other studies [15, 16] no doublet structure for the Pb core levels was observed. According to Morgan and Van Wazer [16], the binding energies for the Pb 4f core levels of PbO, PbO_2 and Pb_3O_4 are all the same. Thomas and Tricker [15] reported differences, with the lowest binding energies found for β-PbO_2 (142.0 and 137.3 eV for $Pb(4f_{5/2})$ and $Pb(4f_{7/2})$, respectively) and for the tetragonal and orthorhombic modifications of PbO, values of 143.3 eV for $Pb(4f_{5/2})$ and 138.6 eV for $Pb(4f_{7/2})$ were found. For Pb_3O_4, intermediate values of 142.3 and 137.5 eV were found. We conclude from these data that there is no clear evidence for a splitting of Pb(4f) core levels in Pb_3O_4 as a result of the presence of two types of Pb atoms.

At room temperature Pb_3O_4 crystallizes in a tetragonal structure with space group $P4_2/mbc$-D_{4h}^{13} [17]. At lower temperatures Pb_3O_4 undergoes a sequence of ferroelastic and ferroelectric phase transitions [18–21]. The low temperature phase, stable below 170 K, has an orthorhombic structure with space group Pbam-D_{2h}^{9}, which is a subgroup of the space group of the high temperature phase. The orthorhombic distortion decreases with increasing temperature and has values $b/a = 0.927$ at 5 K and $b/a = 0.968$ at 140 K. At 170 K the low temperature structure transforms into a non-centrosymmetric pseudo-quadratic structure with symmetry 2 mm; the orthorhombic distortion of this phase is very small, with a value $b/a = 0.998$ at 180 K. At

195 K there is a transition to a non-centrosymmetric tetragonal phase with symmetry 4mm. Finally, this phase transforms into the centrosymmetric tetragonal room temperature structure at 225 K. In all these phases, the atomic positions are close to the positions in the high temperature tetragonal phase; the phase transitions correspond to small shifts of the atoms.

Two types of lead atoms with different coordination can be distinguished in the room temperature tetragonal structure. One type is coordinated by six oxygen atoms in the form of a slightly distorted octahedron. The other type of atom is coordinated in a very asymmetric way by an irregular pyramid of four oxygen atoms, with the lead atoms at the vertex. The coordinations are similar to those observed in the oxides PbO, with Pb in a pyramidal coordination of four oxygen atoms and PbO_2 with Pb in an octahedral coordination. This correspondence is traditionally interpreted as (indirect) evidence for the mixed valence character of Pb_3O_4. Therefore, the octahedrally coordinated Pb atoms in Pb_3O_4 are lead atoms with a (formal) valency of IV, like in PbO_2. The lead atoms coordinated by the pyramid have a formal valency of II, like in PbO. The formula for Pb_3O_4 can thus be written as $Pb(II)_2Pb(IV)O_4$.

In this paper we present *ab-initio* calculations of the electronic structure of Pb_3O_4 using the augmented spherical wave (ASW) method. The results are compared with electronic structure calculations for β-PbO and β-PbO_2. This comparison shows that the electronic structures of the two types of lead atoms in Pb_3O_4 correspond very closely to the electronic structures of lead atoms in β-PbO and β-PbO_2. This is direct evidence that Pb_3O_4 is indeed a mixed valence compound.

2. CRYSTAL STRUCTURE

The room temperature phase of Pb_3O_4 has a tetragonal crystal structure with space group $P4_2/mbc\text{-}D_{4h}^{13}$, with $Z = 4$ formula units in the crystallographic unit cell [17]. The unit cell axes at 293 K are $a = 0.8811$ nm and $c = 0.6563$ nm. One type of lead atom, with formal valency Pb(IV), occupies the 4d positions with coordinates $\pm(0,\frac{1}{2},\frac{1}{4};\ \frac{1}{2},0,\frac{1}{4})$. The other type with formal valency Pb(II), occupies the 8h positions with coordinates $\pm(x,y,0;\ \bar{y},x,\frac{1}{2};\ x+\frac{1}{2},\bar{y}+\frac{1}{2},0;\ y+\frac{1}{2},x+\frac{1}{2},\frac{1}{2})$, with $x = 0.140$ and $y = 0.163$. The oxygen atoms occupy the 8g position with coordinates $\pm(x,x+\frac{1}{2},\frac{1}{4};\ x,x+\frac{1}{2},\frac{3}{4};\ x+\frac{1}{2},\bar{x},\frac{1}{4};\ x+\frac{1}{2},\bar{x},\frac{3}{4})$, with $x = 0.671$ and the 8h position with $x = 0.096$ and $y = 0.637$.

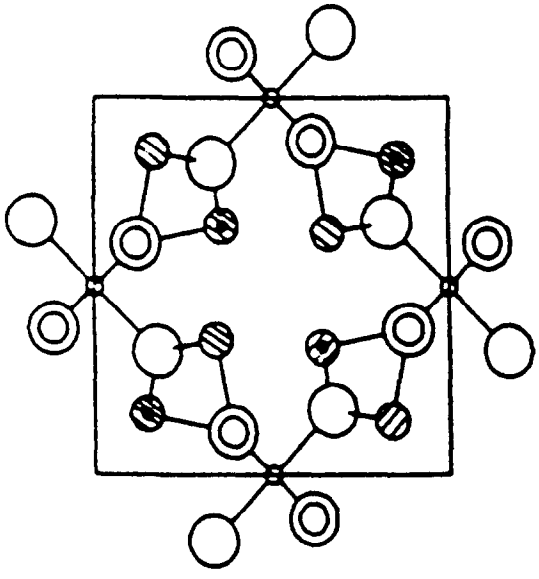

Fig. 1. Structure of Pb_3O_4 projected on the ab plane. The small circles represent the Pb(IV) atoms, and the hatched circles without and with dots Pb(II) atoms at $z = 0$ and $z = \frac{1}{2}$, respectively. The large open circles are apical oxygen atoms at $z = \frac{1}{4}$ and $z = \frac{3}{4}$ and the double circles are equatorial oxygen atoms at $z = 0$ and $z = \frac{1}{2}$.

The structure consists of chains of PbO_6 octahedra which share common edges and which extend in the direction of the c-axis (see Fig. 1). Additional Pb(II) atoms form bridges between the chains of octahedra. Each Pb(II) atom is close to one oxygen in an equatorial edge and to two other oxygen atoms not in

Table 1. Interatomic distances (in nm) in Pb_3O_4, β-PbO_2 and β-PbO

Distance type	Pb_3O_4	β-PbO_2	β-PbO
Pb(IV)–O	0.220 (x4)	0.2169 (x4)	
	0.213 (x2)	0.2149 (x2)	
average Pb(IV)–O	0.218	0.2162	
Pb(IV)–Pb(IV)	0.3282	0.3387	
O–O	0.288	0.2711	0.2944
	0.293	0.3053	0.3030
	0.3282	0.3387	0.3171
Pb(II)–O	0.2215 (x2)		0.2221
	0.2337		0.2249
	0.273		0.2481 (x2)
average Pb(II)–O	0.2374		0.2358
Pb(II)–Pb(II)	0.379		0.3536

Table 2. Input parameters for the band-structure calculation of Pb_3O_4

Atom	Start configuration	R_{WS} (pm)	Atomic position
Pb(IV)	$[Xe]4f^{14}5d^{10}6s^26p^2$	152.4	4d
Pb(II)	$[Xe]4f^{14}5d^{10}6s^26p^2$	158.7	8h ($x = 0.140$, $y = 0.163$)
O1	$[He]2s^22p^4$	105.3	8g ($x = 0.671$)
O2	$[He]2s^22p^4$	104.2	8h ($x = 0.096$, $y = 0.637$)
ES1	$1s^02p^0$	152.4	4b
ES2	$1s^02p^0$	124.4	8g ($x = 0.181$)
ES3	$1s^02p^0$	153.9	8h ($x = 0.663$, $y = 0.626$)

equatorial edges. These latter apical oxygen atoms are in adjacent octahedra of the same chain. The equatorial oxygen forms part of a neighbouring chain and the Pb(II) atoms form the border of large channels parallel to the c-axis.

In Table 1 the interatomic distances in Pb_3O_4 are compared with the distances in β-PbO [22] and β-PbO_2 [23]. The average Pb–O distances for Pb(II) and Pb(IV) in Pb_3O_4 are only 1% larger than in PbO and PbO_2, respectively. However, the distortions of the $Pb(IV)O_6$ octahedra and the tetragonal $Pb(II)O_4$ pyramids in Pb_3O_4 is much larger than in the simple oxides.

3. BAND STRUCTURE CALCULATIONS

Self consistent band structure calculations were performed using the augmented spherical wave (ASW) method [24]. Exchange and correlation were treated within the local density approximation [25]. Scalar relativistic effects were included as described by Methfessel and Kübler [26]. To take into account the spin orbit interaction, an extra term $\lambda \underline{L}.\underline{S}$ was incorporated in the Hamiltonian.

In the ASW method the crystal is subdivided into Wigner–Seitz spheres surrounding the atoms. Within each sphere the potential is taken spherically symmetric; this so-called muffin–tin approximation has proven to give reliable results for close-packed structures. Due to the presence of the asymmetrically coordinated Pb(II) atoms and the presence of large channels, the structure is far from being close packed. A better approximation of the true crystal potential of more open structures can be obtained by filling the unoccupied space with so-called empty spheres (ES). For the calculations on Pb_3O_4, three types of ES were included. The positions and Wigner–Seitz radii (R_{WS}) of the ES are listed in Table 2, together with the Wigner–Seitz radii of the atoms. The empty sphere at the 4b position, ES1, is situated in the middle of the channels and the second type of empty sphere at the 8g position is located inside the PbO_4 pyramids. The Pb(IV) atoms are only surrounded by two empty spheres with a distance Pb(IV)-ES2 = 0.225 nm ($2x$). Each Pb(II) is coordinated by seven empty spheres at the following distances: Pb-ES1 = 0.2505 nm ($2x$), Pb-ES2 = 0.2283 nm ($2x$) and Pb-ES3 = 0.2690, 0.2554 and 0.2543 nm. This large coordination of Pb(II) by empty spheres will have implications when the charges on the atoms are considered; a large part of electronic charge in the empty spheres should be assigned to Pb(II) atoms.

For the ASW calculations we used a basis set consisting of 6s, 6p and 6d functions for Pb and 2s and 2p functions for O and 1s and 2p functions for the empty spheres. Pb 5f and O 3d functions were included in the internal summation of the three center contributions to the matrix elements, which can be interpreted as taking these functions as a perturbation. The choice of basis functions implies that the effect of hybridization of Pb 5d with O 2s is not taken into account. This hybridization is quite strong because the orbital energies of Pb 5d and O 2s are nearly the same, but the effect of Pb 5d/O 2s hybridization on the valence and conduction bands and the chemical bonding is small [27].

The Brillouin zone of the tetragonal room temperature phase of Pb_3O_4 is shown in Fig. 2. The calculated energy bands along symmetry lines are presented in Fig. 3; we have used the symmetry notations of Miller

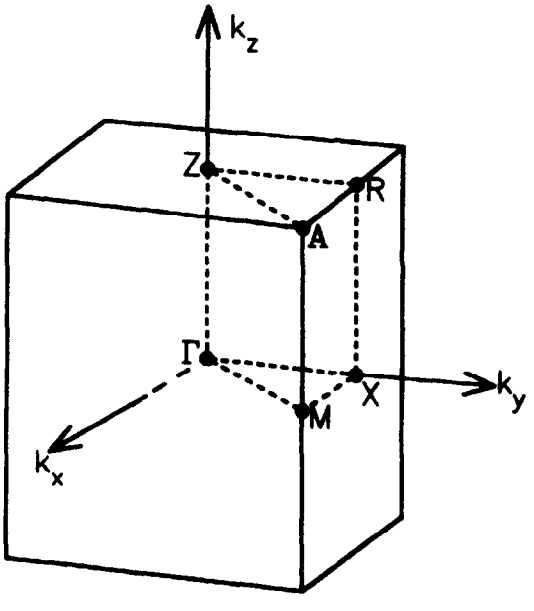

Fig. 2. Brillouin zone of tetragonal Pb_3O_4.

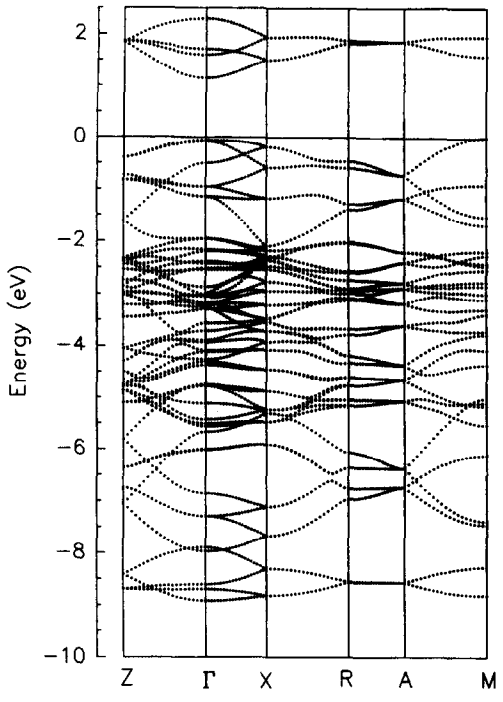

Fig. 3. Energy bands of Pb_3O_4 calculated with the ASW method, including spin-orbit interaction.

and Love [28]. Figure 4 shows the total and partial density of states and in both Figs 3 and 4, the top of the valence band has been taken as the energy zero. The charges in the muffin–tin spheres and the orbital configuration of the atoms and empty spheres are listed in Table 3. Generally, not too much significance should be attributed to the charges calculated in this way, because the values of the charge within the Wigner–Seitz sphere depend strongly on the values used for the Wigner–Seitz radii and on the presence of empty spheres. The charge within the Wigner–Seitz sphere cannot be identified with the ionic charge. This is clearly demonstrated by the remarkable fact that the positive charge in the Wigner–Seitz sphere of Pb(II) is larger than that of Pb(IV). The reason is that a considerable amount of electronic charge, located in the empty spheres surrounding Pb(II), should be assigned to the atomic charge of Pb(II).

The valence band region consists of 56 energy bands and has a width of 9.0 eV. The maximum of the valence bands is at M, but this maximum is only 0.06 eV higher in energy than the maximum at Γ. The lowest four bands, ranging from −8 eV to the bottom of the valence bands, mainly consist of 6s states of Pb(IV) mixed with O 2p states (Fig. 4). The next eight bands between −6 and −8 eV have mainly Pb(II) 6s character with some hybridization with O 2p states. Four of these bands show a large dispersion of about 2 eV in the Γ–Z direction. The next 36 bands between −6 and −2 eV are the (nearly non-bonding) O 2p states, mixed slightly with Pb(IV) 6p states; these bands have a small dispersion throughout the whole Brillouin zone. The top eight bands, with a total width of 2.3 eV, are predominantly Pb(II) 6s in character, mixed with O 2p states. The hybridization of Pb(IV) 6s and O 2p orbitals is very strong, resulting in a distribution of Pb(IV) states over two energy bands at −9 eV and +2 eV, i.e. separated by 11 eV. Such a very strong Pb(IV) 6s – O 2p hybridization is also present in β-PbO_2 [29] and $BaPbO_3$ [30]. Hybridization of Pb(II) 6s with O 2p orbitals is also strong and gives rise to bands between −8 and −5 eV and −2 and 0 eV.

The bottom of the conduction band is at Γ. According to our calculations Pb_3O_4 is a semiconductor with an indirect energy gap of 1.1 eV. The

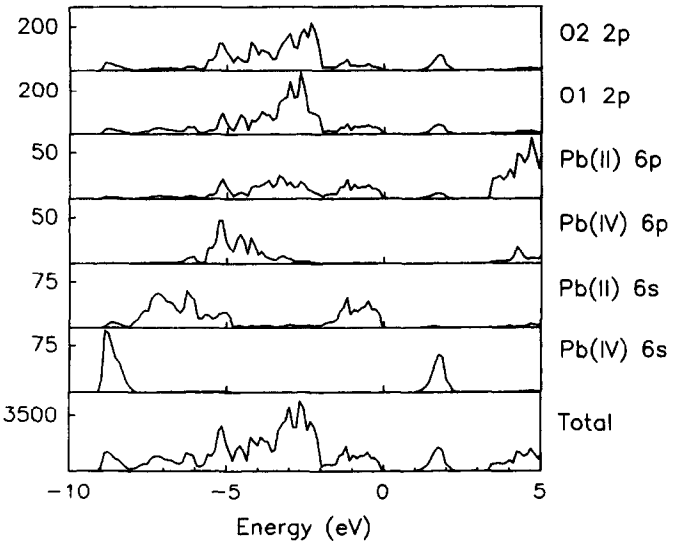

Fig. 4. Total and partial density of states of Pb_3O_4. Units: total DOS: states/(Ry.unit cell); partial DOS: states/(Ry.atom).

Table 3. Charges in the Wigner–Seitz spheres and atomic configuration of atoms and empty spheres for Pb_3O_4

Atom	Charge	Configuration
Pb(IV)	+0.73	$6s^{1.12}6p^{1.21}6d^{0.69}5f^{0.24}$
Pb(II)	+1.30	$6s^{1.53}6p^{0.73}6d^{0.28}5f^{0.16}$
O1	+0.08	$2s^{1.69}2p^{4.22}3d^{0.01}$
O2	+0.13	$2s^{1.69}2p^{4.17}3d^{0.02}$
ES1	−0.58	$1s^{0.23}2p^{0.25}3d^{0.10}$
ES2	−0.78	$1s^{0.26}2p^{0.33}3d^{0.19}$
ES3	−0.79	$1s^{0.23}2p^{0.33}3d^{0.22}$

calculated direct energy gap is at Γ, with a value of 1.2 eV. The lowest conduction band consists of four energy bands with mainly Pb(IV) 6s character, mixed with O 2p states. This conduction band is narrow, and has a total width of 1.3 eV.

The large contribution of Pb(IV) 6p orbitals to the charge density of the valence bands (see Fig. 4 and Table 3), indicates that the bonds between Pb(IV) and oxygen are strongly covalent. The divalent lead atoms and oxygen atoms form bonds which are more ionic in character.

4. DISCUSSION

The only electronic structure calculation for Pb_3O_4 reported in literature, was performed by Evarestov and Veryazov [31], using the semi-empirical LUC-CNDO method. These authors give only the total density of states and the eigenvalues at Γ and their results differ strongly from our calculations. The valence band width is smaller and the shape of the valence band density of states curve is also quite different and they find a sharp peak at the bottom of the valence band which they ascribe to Pb 6s states. We think that our calculation is more reliable, as it uses a more advanced method without adjustable parameters.

By comparing the electronic structure of Pb_3O_4, calculated with the ASW method (Figs 3 and 4), with the electronic structure reported for α- and β-PbO [32] and β-PbO_2 [29], we observe great similarities. The partial density of states of Pb(II) atoms in Pb_3O_4 is very similar to that of Pb(II) in PbO and consists of a distribution of Pb(6s) states over two energy bands, one between −8 and −5 eV, and one between −2 and 0 eV. The partial density of states of the Pb(IV) atoms in Pb_3O_4 is very similar to that of Pb(IV) atoms in β-PbO_2, with the Pb(6s) states distributed over two bands 11 eV apart. This clearly shows that the electronic structures of the two types of lead atoms in Pb_3O_4 are nearly the same as the lead atoms with (formal) valencies II and IV in PbO and PbO_2, respectively and proves that Pb_3O_4 is indeed a mixed valence compound.

A characteristic of Pb(II) atoms in oxides is the presence of a so-called lone pair of electrons which is responsible for the asymmetric coordination of Pb(II) [33, 34]. The lone pairs occupy the empty space in the crystal lattice near the Pb(II) atoms opposite to the four coordinating oxygen atoms. For Pb_3O_4 this corresponds to the empty channels: the lone pairs of Pb(II) stick out into the channels. Le Bellac [35] has discussed the structures and phase transitions of Pb_3O_4 using an electrostatic model. The Pb(II) atoms are highly polarizable and the asymmetric coordination by oxygen ions induces a large dipole moment on Pb(II). This polarization of Pb(II) corresponds to the lone pair of electrons extending at one side of the Pb(II) atoms, in the direction of the channels; the phase transitions of Pb_3O_4 are attributed to small changes of the orientation of the lone pairs.

According to our calculations, Pb_3O_4 is a semiconductor with a band gap of 1.1 eV. This value is smaller than the experimentally observed band gap of 2.1–2.2 eV. This is a common defect of many electronic structure calculations using the LD approximation.

The top of the valence band of Pb_3O_4 consists mainly of Pb(II)(6s) states, the bottom of the conduction band of Pb(IV)(6s) states. Therefore, conduction in p-type semiconducting Pb_3O_4 will be due to holes in the Pb(II)6s band, which corresponds to Pb^{3+} ions on the Pb(II) sites. Conduction in *n*-type Pb_3O_4 is due to electrons in the Pb(IV) 6s band, corresponding to Pb^{3+} ions on the Pb(IV) sites. Thus optical excitation of an electron from the top of the valence band to the bottom of the conduction band corresponds to an intervalence charge transfer transition $Pb^{2+} + Pb^{4+} + h\nu \rightarrow Pb^{3+} + Pb^{3+}$. (We remark that this is a strongly simplified picture, because of the strong hybridization of Pb(6s) and O(2p) states.)

Acknowledgements—This work is part of the research program of the Stichting voor Scheikundig Onderzoek Nederland (SON) and the Stichting voor Fundamenteel Onderzoek der Materie (FOM), which are financially supported by the Nederlandse Organisatie voor Wetenschappelijk Onderzoek (NWO).

REFERENCES

1. Schuster, H. J., *Chem. Ing. Techn.* 1956, **28**, 654.
2. Kumar, S., Sharon, M. and Jawelekar, S. R., *Thin Solid Films*, 1991, **195**, 273.
3. McDewitt, M. T. and Brown, W. L., *Spectrochimica Acta*, 1964, **20**, 799.
4. Oehme, F., *Z. Naturforschung*, 1959, **14b**, 779.
5. Oehme, F., *Chemiker Zeitung*, 1961, **44**, 170.
6. Keester, K. L. and White, W. B., *Mat. Res. Bull.*, 1969, **4**, 757.
7. Pamfilov, A. V., Evanchevka, E. G. and Drogomeretskie, P. V., *Russ. J. Phys. Chem.*, 1967, **41**, 565.
8. Sharon, M., Kumar, S., Sathe, N. P. and Jawelekar,

S. R., in *Renewable energy sources*, ed. T. N. Veziroglu. Elsevier, Amsterdam, 1984, p. 321.
9. Sharon, M., Kumar, S., Sathe, N. P. and Jawelekar, S. R., *Solar Cells*, 1984, **12**, 353.
10. Sharon, M., Kumar, S. and Jawelekar, S. R., *Bull. Mater. Sci.*, 1986, **8**, 415.
11. Kumar, S., Sharon, M. and Jawelekar, S. R., *Ind. J. Chem.*, 1989, **28A**, 752.
12. Benschop, F. J. M., thesis, Leiden, 1993.
13. Benschop, F. J. M., Brom, H. B., Zandbergen, H. W. and Cava, R. J., *Physica*, 1994, **235/240**, 2527.
14. Kim, K. S., O'Leary, T. J. and Winograd, N., *Anal. Chem.*, 1973, **45**, 2214.
15. Thomas, J. M. and Tricker, M. J., *J. Chem. Soc. Faraday II*, 1975, **71**, 329.
16. Morgan, W. E. and Wazer, J. R. van, *J. Phys. Chem.*, 1973, **77**, 964.
17. Gavarri, J. R. and Weigel, D., *J. Solid State Chem.*, 1975, **13**, 252.
18. Gavarri, J. R., Calvarin, G. and Weigel, D., *J. Solid State Chem.*, 1975, **14**, 91.
19. Gavarri, J. R. and Weigel, D., *J. Solid State Chem.*, 1978, **23**, 327.
20. Garnier, P., Calvarin, G. and Weigel, D., *J. Solid State Chem.*, 1976, **16**, 55.
21. Garnier, P., Calvarin, G. and Weigel, D., *J. Solid State Chem.*, 1978, **26**, 357.
22. Hill, R. J., *Acta Cryst.*, 1985, **C41**, 1281.
23. Hill, R. J., *Mat. Res. Bull.*, 1982, **17**, 769.
24. Williams, A. R., Kübler, J. and Gelatt Jr., C. D., *Phys. Rev.*, 1979, **B19**, 6094.
25. Barth, U. von, and Hedin, L., *J. Phys.*, 1972, **C5**, 1629.
26. Methfessel, M. and Kübler, J., *J. Phys.*, 1982, **F12**, 141.
27. Terpstra, H. J., thesis, Groningen, 1996.
28. Tables of Irreducible Representations of Space Groups and Corepresentations of Magnetic Space Groups, Pruett, Boulder, 1967.
29. Heinemann, M., Terpstra, H. J., Haas, C. and De Groot, R. A., *Phys. Rev.*, 1995, **B52**, 11 740.
30. Mattheis, L. F. and Hamann, D. R., *Phys. Rev.*, 1982, **B26**, 2686.
31. Evarestov, R. A. and Varyazov, V. A., *Phys. Stat. Sol.* (b), 1991, **165**, 401.
32. Terpstra, H. J., De Groot, R. A. and Haas, C., *Phys. Rev.*, 1995, **B52**, 11 690.
33. Orgel, L. E., *J. Chem. Soc.*, 1959, 3815.
34. Galy, J, Meunier, G., Andersson, S. and Åström, A., *J. Solid State Chem.*, 1975, **13**, 142.
35. Le Bellac, D., Kiat, J. M. and Garnier, P., *J. Solid State Chem.*, 1995, **114**, 459.